A Merging Criterion for Two-dimensional Co-rotating Vortices

Patrice Meunier,[1] Uwe Ehrenstein,[2] Thomas Leweke,[1] and Maurice Rossi[3]

[1]*Institut de Recherche sur les Phénomènes Hors Équilibre, UMR 6594 CNRS/Universités Aix-Marseille, 49 rue F. Joliot-Curie, B.P. 146, F-13384 Marseille Cedex 13, France*

[2]*Laboratoire J.-A. Dieudonné, Université de Nice - Sophia Antipolis, Parc Valrose, F-06108 Nice Cedex 02, France*

[3]*Laboratoire de Modélisation en Mécanique, Université de Paris VI, 4 place Jussieu, F-75252 Paris Cedex 05, France*

(Dated: January 3, 2002– revised version)

Abstract

We propose a quantitative criterion for the merging of a pair of equal two-dimensional co-rotating vortices. A cross-validation between experimental and theoretical analyses is performed. Experimental vortices are generated by the roll-up of a vortex sheet originating from the identical and impulsive rotation of two plates. The phenomenon is then followed up in time until a rapid pairing transition occurs for which critical parameters are measured. In the theoretical approach, the nonlinear Euler solution representing a pair of equal vortices is computed for various nonuniform vorticity distributions. The stability analysis of such a configuration then provides critical values for the onset of merging. From this data set, a criterion depending on global impulse quantities is extracted for different shapes of the vorticity distribution. This theoretical statement agrees well with our experimentally based criterion.

I. INTRODUCTION

The pairing process of vortices is one of the main building blocks of fluid motion and plays a major role in a variety of fluid phenomena: decaying two-dimensional turbulence [1–4], three-dimensional turbulence [5–7], and mixing layers [8, 9], to name a few. Its potential significance covers various fields such as geophysics, meteorology, and astrophysics.

The simplest case of interaction, *i.e.* a pair of equal vortices, possesses recurrent features [10, 11]. When they are far apart, their time evolution is close to the dynamics of two point vortices rotating around each other with a turnover period $2\pi^2 L^2/\Gamma$, which depends only on their circulation Γ and separation distance L. In addition, a weaker effect is generated by the local strain produced by one vortex on its companion: an elliptic deformation of the streamlines and vorticity contours [12]. In addition to these two effects, which are mainly caused by inviscid interactions, an increase of the vortex radius is observed due to viscous diffusion of vorticity. This induces a simultaneous increase of the ratio between the vortex radius and the separation distance. This quantity may also be changed by the presence of a third vortex in the neighborhood of the vortex pair. In any case, an abrupt modification arises when this aspect ratio reaches a critical value: the vortices start to eject tips of vorticity in their outer region. These structures then grow into filaments wrapping around the pair. In about one turnover period, the fusion (or merging) of both vorticity regions is achieved, giving rise to a unique and bigger vortex with filamentary structures around it [13, 14].

In this context, it is worth focussing on quantitative aspects of each phase: the first stage may be understood within a two-dimensional asymptotic analysis [4, 12], although a three-dimensional elliptic instability may arise complicating the picture of dynamics before merging [11]. The merging process itself is a highly nonlinear process that can be analyzed through numerical simulations [13] or analytical means [15]. An important point concerns the onset of merging. It has previously been argued [16] that the merger process may be viewed as an instability of a pair of vortices. In this context, the computation of nonlinear equilibria between two vortices and the study of their stability are necessary steps. The present paper is based on such a theoretical background, the validity of which is supported by comparisons between experimental and theoretical results.

Most previous attempts have focussed on constant-vorticity patches. Let us mention the works by Saffman and Szeto [17], Dritschel [16, 18], Overman [19] and Waugh [20]. Such approximations are extremely valuable, but comparisons with experiments should preferably be done using results obtained with non-uniform vorticity distributions, since experimental vortices are

definitively closer to such cases. For instance, vortices in two dimensional turbulence are better approximated by Lamb–Oseen vortices with a Gaussian vorticity profile [4]. Only recently, solutions for such a non-uniform case have been computed *via* a nonlinear continuation procedure [23]. In the present work, this tool, which provides numerically a relationship between streamfunction and vorticity, is used to investigate the proper non-dimensional parameters determining the onset of merging. Such characteristics could then possibly be introduced in simplified model equations describing two-dimensional turbulence. Using a theory of equilibrium statistical mechanics, Robert and Sommeria [21] and Turkington [22] have shown, for instance, that organized structures in two-dimensional turbulence are steady solutions of the Euler equations, characterized by an explicit relationship between streamfunction and vorticity.

The paper is organized as follows. In section II, the experimental set-up is briefly described, and the evolution of a co-rotating vortex pair is analyzed, leading to an experimental criterion for the onset of merging. We formalize, in section III, the nonlinear method which allows the computation of Euler solutions of co-rotating vortices with non-uniform vorticity distribution. In section IV, the instability point of such a configuration, which is interpreted as a sign for the onset of merging, is computed for various vortex shapes. Focussing on a general merging criterion, a particular dimensionless parameter is introduced and compared for the various initial vortex shapes under consideration, also with the experimental findings.

II. THE PAIRING EXPERIMENT

A. Set-up

Two identical vortices are generated in a water tank using two flat plates with sharpened edges, impulsively started from rest in a symmetric way. The rotation of the plates around their vertical axes creates two starting vortices, which are laminar, two-dimensional, and without axial velocity in the observation volume. The temporal evolution of the flow is visualized using two different dyes, illuminated by an Argon ion laser. Digital Particle Image Velocimetry (DPIV) is used for quantitative velocity measurements (see [11] for further details).

The vortex pair is characterized by the circulation Γ of each vortex, the separation distance L_o between the two vortex centers (given by the local maxima of vorticity) and the core size a, found

by a least-squares fit of the measured vorticity to the theoretical distribution of a Gaussian vortex:

$$\omega = \frac{\Gamma}{\pi a^2}\ e^{-r^2/a^2}. \tag{1}$$

Measurements have shown that this profile is a fairly accurate representation of the experimental vortices in the initial stages of the flow. Pairs of such vortices are characterized by two non-dimensional parameters: the Reynolds number $Re = \Gamma/\nu$, where ν is the kinematic viscosity, and the non-dimensional core size a/L_o.

In a viscous flow, the core radius a grows in time by diffusion of vorticity according to:

$$a^2 = 4\nu t + \text{const.} \tag{2}$$

Time t is non-dimensionalised here by the turnover period $T = 2\pi^2 L_o^2/\Gamma$ of a point vortex pair having the same circulation and (initial) separation distance as the pair under consideration. The origin of time is chosen so that the constant in Eq. (2) vanishes, *i.e.* it corresponds to a hypothetical time when the the flow consists of two point vortices. The non-dimensional time thus defined is denoted by t^*. In the viscous case, the overall evolution of the flow therefore depends only on the Reynolds number, which in the present set of experiments varied between 700 and 2300.

B. Dye visualizations

The experimental merging of two distributed vortices is illustrated in Fig. 1, which presents cross-cut visualizations of the flow at different stages, giving a qualitative overview of the vortex pair evolution. For a more precise characterization, a quantitative analysis was carried out using DPIV measurements [24], which confirmed and validated the description of the phenomenon which follows.

In a first stage (after vortex formation, which is not considered in further detail here), the vortices are far enough apart to remain practically axisymmetric (Fig. 1a). (The spiral structure seen in these visualizations is not representative of the vorticity distribution at these low Reynolds numbers; the vorticity diffuses and smooths out much more rapidly than the dye, leading to a vorticity field close to (1) at early times). As their core sizes increase due to viscosity, they deform in an elliptic way (Fig. 1b), and create a tip on their inner side. Each tip is attracted by the opposite vortex, but the separation between the two centers still remains approximately constant (see Fig. 2). During this stage, the core size a closely follows the evolution (2) for an isolated Gaussian vortex.

When the core size reaches a critical fraction of the separation distance, a second stage begins, in which the two vortices rapidly get closer and finally merge into a single pattern that has some resemblance with the Chinese Yin-Yang symbol (Fig. 1c). The critical ratio a_c/L_o at which the separation distance begins to decrease was previously found to be approximately 0.26 [24]. However, this criterion (the start of the decrease of L) is somewhat subjective, since the evolution of the separation distance is continuous and gradual. Below we propose an alternative way to calculate the critical core size more objectively. The second stage, *i.e.* the merging itself, seems to be mainly a convective process, since the decrease of the separation distance L is fairly independent of the Reynolds number. During this stage, two arms of dye are ejected and roll up around the central pattern, forming a spiral of dye in Fig. 1(d), representative of a spiral of vorticity. In a final third stage, these spirals are stretched and are more and more entangled together by differential rotation. This leads to an axisymmetrization of the final vortex, when the distance between two spirals decreases down to the order of the diffusion length of the vorticity.

C. Determination of the critical core size

The evolution of the separation distance L plotted in Fig. 2 does not show a sharp transition between the two first stages mentioned above. In particular, the point at which the distance L starts to decrease, is not precisely identifiable on the curve. It is thus difficult to determine accurately the beginning of the merging stage from such a measurement. However, a quantitative criterion identifying this point would be of importance in the dynamics of multiple-vortex systems, if one is interested to know under which conditions two vortices approaching each other will merge or, alternatively, continue on their initial trajectories without strong interaction. The combined treatment of the data of seven experiments, carried out at different Reynolds numbers, allowed us to find the more accurate criterion presented below.

The first stage of the evolution of two co-rotating vortices is mainly governed by viscous diffusion. Taking into account the choice for the origin of time given above, equation (2) can be rewritten in non-dimensional form as

$$\left(\frac{a}{L_o}\right)^2 = \frac{8\pi^2}{Re}\, t^*, \tag{3}$$

which gives a theoretical prediction for the evolution of the ratio of core size and separation distance. This ratio has been measured experimentally [24], and good agreement with (3) was found.

We can now find an expression for the time t_c^* at which the vortex pair reaches the critical ratio a_c/L_o:

$$t_c^* = \left(\frac{a_c}{L_o}\right)^2 \frac{Re}{8\pi^2} \equiv A\,Re \tag{4}$$

which is proportional to the Reynolds number: the less diffusion acts, the longer it takes to reach the critical core size.

For the present purpose, the second stage (the actual merging) is now assumed to be a purely convective process, based on the observation that the evolution of the separation distance L during this stage is fairly independent of the Reynolds number. The laps of time, in convective units, needed for the separation distance L to decrease from its initial value L_o to a certain percentage x of L_o is therefore assumed to be a quantity B_x, depending only on x, and not on Re. The value of x to be taken is of course somewhat arbitrary. Values of x in the range 30–80% have been considered: measurements could hardly provide reliable values for x below the lower bound, and for ratios L/L_0 close to unity it is not certain if merging has really started or not.

Adding this to the critical time t_c^* in (4), we obtain an expression for the time t_x^* at which the separation distance L has reached a fraction x of its initial value:

$$\tilde{t}_x^* = A\,Re + B_x. \tag{5}$$

As an example, the experimental measurements of t_x^* as function of Reynolds number is shown in Fig. 3 for $x = 60\%$. The variation is indeed found to be linear in Reynolds number, which validates our two-stage model for the interaction of two co-rotating vortices. The slope A, which is found from a least-squares fit to the data, provides the critical non-dimensional core size a_c/L_o (see Eq. (4)).

The advantage of this procedure lies in the fact that we can use experimental measurements of the separation distance *anywhere* during the merging phase, in particular during the initial stage when L is still fairly high and the measurements are reliable. Towards the end of merging, when L falls down to zero, the uncertainty of L, which is obtained from DPIV velocity fields, is much larger.

The critical core size was determined for different values of x, and the results are plotted in Fig. 4. A slight variation of a_c/L_o with x is observed, which is however within the experimental uncertainty. From these measurements, an experimental merging criterion can be established for two co-rotating vortices with an approximately Gaussian vorticity distribution: merging occurs

when the rescaled core radius a/L_o exceeds a critical value given by

$$\left(\frac{a_c}{L_o}\right) = 0.24 \pm 0.01. \tag{6}$$

This critical value is slightly smaller than the one announced in a previous paper [24], where $a_c/L_o = 0.26 \pm 0.01$. In this analysis, the value was measured at the instant when the separation distance starts to decrease, *i.e.* somewhat *after* the beginning of the second stage, and led to a higher estimation of the critical ratio. Nevertheless, the new value is still close, the small difference can be considered as a correction to the previous result, obtained in a more objective way, and less sensitive to measurement noise and uncertainty.

An example of the vorticity distribution measured at the critical time t_c^* is shown in Fig. 5 for $Re = 1506$. The flow is just about to lose its symmetry with respect to the center point, by the formation of outer tips in the pattern, similar to what is observed in the dye visualisation of Fig. 1(b).

III. THEORETICAL APPROACH: COMPUTATION OF NONLINEAR EULER SOLUTIONS AND THEIR STABILITY

Due to the rapid nature of this transition, the merging phase may be considered as an inviscid process, at least at onset. Clearly, viscosity becomes important when sufficiently high gradients are produced later on by the roll-up, in a way described in [25] or [26]. In the following, the flow is thus assumed incompressible and inviscid.

Contour dynamics approaches have successfully been applied to the computation of equilibria of vortex patches [16, 18, 20, 27]. In the present investigation, two identical vortices with several vorticity distributions are considered, ranging from the classical patches of vorticity to Gaussian or parabolic profiles. Generalizing the numerical procedure used by Saffman & Szeto [17] to compute equilibria of vortex patches, the perturbed streamlines are computed, using Green's function integrals. For self-consistency, we first briefly present the numerical algorithm used to compute the equilibrium configurations for interacting vortices with general vorticity profiles. More details about the numerical procedure may be found in [23]. For the computation of the nonlinear equilibria of two identical co-rotating vortices (see Fig. 6 for the configuration), the basic idea is as follows: when the vortices are far apart, *i.e.* when the distance L between their centers is much greater than the characteristic vortex radius, the local strain induced by the companion vortex may

be neglected. Each vortex may be taken as axisymmetric, with an outer boundary at $r = r_m$, and rotating with a frequency $\Gamma/(\pi^2 L^2)$ around the center O of the flow. For symmetry reasons, O is located at equal distances to both vortices. Moreover, each vortex is characterized by a given vorticity profile, which can be chosen arbitrarily, with the proviso that its maximum is located at the center of isovorticity contours, denoted by O_i for a given vortex i ($i = 1, 2$). Note that this condition must be verified for centrifugally stable vortices [28]. The circular streamlines of the unperturbed isolated vortices are hence parameterized by their radial position, which is a function of vorticity: $r_{o,i}(\omega_i)$. When the vortices get closer to each other, the streamlines are deformed, and vorticity contours ω_i now lie on lines given by

$$r_i(\omega_i, \theta) = \sqrt{r_{o,i}^2(\omega_i) + f_i(\omega_i, \theta)}, \quad 0 \leq \theta \leq 2\pi, \quad i = 1, 2, \tag{7}$$

where r_i is again measured from the vortex center O_i. By decreasing the distance L step by step, we use a nonlinear continuation procedure to follow the solution of a pair of vortices, using as a starting point the previous axisymmetric solution and a large parameter L. This method is standard in nonlinear problems when one looks for fixed points of dynamical systems [29]. In the present case, the unknown variables consist of functions $f_i(\omega_i, \theta)$ for one vortex, *e.g.* $i = 1$ (the other one being its symmetric image), and the vortex pair angular frequency Ω. The continuation parameter is the distance between centers: $L \equiv |\overrightarrow{O_2 O_1}|$. The nonlinear constraints are defined as follows. The equilibrium Euler solution is steady in the reference frame rotating with the vortex pair at an angular frequency Ω. The specific contribution of each vortex to the streamfunction reads

$$\psi_i(\mathbf{r}) = -\frac{1}{4\pi} \int_{S_i} \log\left(\left|\mathbf{r} - \mathbf{r}_i'\right|^2\right) \omega_i(\mathbf{r}_i') dS_i', \tag{8}$$

where $\mathbf{r}$ and $\mathbf{r}_i'$ are computed from the center O_i of vortex i and integration is done over the vortex area S_i. This Green's integral can be expressed as a vorticity integral using relation (7)

$$\psi_i(\mathbf{r}) = -\frac{1}{4\pi} \int_{\omega_{min}}^{\omega_{max}} \int_0^{2\pi} \log\left(\left|\mathbf{r} - \mathbf{r}_i(\omega_i', \theta')\right|^2\right) \frac{1}{2}\omega_i' \left(-\frac{\partial r_i^2}{\partial \omega_i}(\omega_i', \theta')\right) d\omega_i' d\theta'. \tag{9}$$

It is assumed that two distinct streamlines never cross each other in the continuation procedure. The total streamfunctions now read

$$\psi_{t,1}(\mathbf{r}_1) = \psi_1(\mathbf{r}_1) + \psi_2(\mathbf{L} + \mathbf{r}_1) + \frac{1}{2}\Omega \left|\frac{1}{2}\mathbf{L} + \mathbf{r}_1\right|^2 \tag{10}$$

$$\psi_{t,2}(\mathbf{r}_2) = \psi_2(\mathbf{r}_2) + \psi_1(-\mathbf{L} + \mathbf{r}_2) + \frac{1}{2}\Omega \left|-\frac{1}{2}\mathbf{L} + \mathbf{r}_2\right|^2, \tag{11}$$

where $\mathbf{L} \equiv \overrightarrow{O_2O_1} = (L, 0)$, and $\mathbf{r}_i$ denote vectors with origin at O_i. A steady solution of the Euler equations must satisfy the straightforward constraint that isovorticity contours must be streamlines. The total stream function is thus constant on each vorticity level, which may be written as

$$\psi_{t,i}(\omega_i, \theta) = C_i(\omega_i), \quad 0 \leq \theta \leq 2\pi, \quad i = 1, 2. \tag{12}$$

One more condition must be added to determine Ω as a function of the distance between the vortex centers. This is achieved by imposing that, in the rotating frame of reference, the vortex centers be stagnation points. This requirement gives one extra condition (by symmetry, case $i = 1$ and $i = 2$ provide an equivalent condition):

$$\lim_{r_i \to 0} \frac{\partial \psi_{t,i}}{\partial r_i}(r_i, \theta = 0) = 0, \quad i = 1, 2, \tag{13}$$

the derivatives of the total stream functions with respect to θ being zero at $\theta = 0$, due to the symmetry with respect to the x-axis. Once vorticity integrals are discretized using Fourier collocation in θ and Chebyshev collocation in ω, together with quadrature rules for the integrals [23], equations (12) and (13) define a fixed point for a large nonlinear system with the continuation parameter L, which is solved using an arclength continuation procedure. [29] For each such equilibrium state, the Jacobian matrix is computed. The nonlinear parameterized system undergoes a bifurcation or a limit point, when the Jacobian matrix has a zero eigenvalue at a (critical) value of the continuation parameter L_c. Those critical points are given as a by-product of the continuation procedure. A discretization using 18 Chebyshev-collocation points in ω and 48 Fourier-collocation points in θ (leading to a nonlinear system of almost 820 equations using the symmetry condition with respect to the x-axis) proved to be sufficient to provide the critical parameter values up to three digits.

IV. TOWARDS A MERGING CRITERION

Various equilibrium configurations have been computed each one corresponding to a specific non uniform axisymmetric profile for $L \gg r_m$. Most of the criteria for merging proposed so far, based on equilibrium solutions of the Euler equations, use uniform vortex patches in the theoretical model. The present method is capable of computing equilibrium states with continuous initial vorticity distributions. In order to be meaningful a merging criterion should not depend on a specific initial axisymmetric profile. We have mainly considered two types of distributions: Lamb-like vortices with vorticity jumps at the outer boundary (uniform patches appear as a limit case), as well as various parabolic profiles.

The system is made dimensionless, such that both vortex types have a circulation $\Gamma = \pi$ and an area $S = \pi$. This implies that the radius of the vortex boundary is taken to be the reference length ($r_m = 1$), and that the vorticity scale depends on the profile. Using these scales, the Lamb-like (Gaussian-like) vorticity profile reads:

$$\omega_i(r) = \beta_g \exp(-\alpha r^2), \quad 0 \leq r \leq 1, \tag{14}$$

where β_g is equal to $\alpha/(1-e^{-\alpha})$. The parameter $e^{-\alpha} = \omega_{\min}/\omega_{\max}$ measures the ratio between the vorticity maximum and the minimum located at the outer boundary for each vortex. This profile is known to fit well coherent structures in decaying two-dimensional turbulence [4]. It should be noted, however, that for high values of α the vorticity is strongly concentrated in the center of the finite-size vortex area (of radius unity). As a consequence, this profile is only physically relevant when α is not too large. An example of an axisymmetric vorticity distribution with $\omega_{min}/\omega_{max} = 0.05$ is shown in Fig. 7. A different case is provided by the parabolic profile

$$\omega_i(r) = \beta_p(1-\alpha r^2), \quad 0 \leq r \leq 1, \tag{15}$$

where $\beta_p = 2/(2-\alpha)$ and $1-\alpha = \omega_{\min}/\omega_{\max}$. In Fig. 7, this vorticity distribution is displayed for $\omega_{min}/\omega_{max} = 0.05$. Some computations have also been performed for a compact initial vortex distribution

$$\omega_i = \beta_c \exp\left(\frac{-\alpha}{1-r^2}\right), \quad 0 \leq r \leq 1, \tag{16}$$

(the factor β_c being such that the circulation is equal to π). One example, with $\alpha = 0.1$, for this third initial solution family is shown in Fig. 7.

In a previous work [23], almost uniform vortex patches with a small α ($= 10^{-3}$) for the Gaussian profile were considered. It was checked by comparing with an earlier work of Dritschel [18], that the critical separation distance L_c (for which the Jacobian matrix of the continuation procedure has a zero eigenvalue) coincides with the point, at which the nonlinear equilibrium state becomes unstable with respect to infinitesimal two-dimensional disturbances. In Saffman [10] it is shown that this exchange-type instability, characterized by the appearance of a zero eigenvalue, occurs when total angular impulse J_{tot} (resp. the total energy E_{tot}), defined as

$$J_{tot} = \int \omega(\mathbf{r})|\mathbf{r}|^2 dS, \quad E_{tot} = \int \omega(\mathbf{r})\psi(\mathbf{r}) dS,$$

reaches a minimum (resp. maximum) ($\mathbf{r}$ is here computed from the center of rotation O). This aspect was confirmed in the present work with parabolic or Lamb-like profiles for various values of

the parameter α. As shown in [18], once an unstable equilibrium state is reached, a fast unsteady evolution occurs which may be characterized as merging. In the present computations, when decreasing the vortex separation distance L starting from large values, the exchange of stability happens at a critical distance L_c at which a (real) eigenvalue of the Jacobian matrix goes through zero. Consequently, the equilibrium state loses stability at L_c; in the framework of the present theoretical model we associate it here with the onset of the merging process. Fig. 8 shows the streamline pattern for such a critical state for three cases: a parabolic profile with $\alpha = 1$ (*i.e.* $\omega_{min} = 0$), a Lamb-like profile with $\alpha = 10^{-3}$, which is very close to a vortex patch, and a Lamb-like profile with $\alpha = 2.25$.

These plots can be compared to the experimental result in Fig. 5. An important difference is the fact that the real flow possesses a non-negligible amount of vorticity at and around the central point between the vortices, a feature which cannot be represented in the theoretical formalism adopted here. The gap δ between the vortices decreases for decreasing $\omega_{min}/\omega_{max}$ until $\delta = 0$ for $\omega_{min} = 0$ in the case of the parabolic initial profile (Fig. 8a). The distance δ takes a finite value at criticality in the uniform case (Fig. 8b). For increasing α in the nonuniform Gaussian vorticity distribution, the presence of a zone of high gradients leads to a cusp at the outer boundary where the vorticity is small (Fig. 8c). The stability appears to be sensitive to the vorticity distribution near the outer boundary, a feature which could be related to the experimental observation of a tip of vorticity generated when pairing is initiated (see Fig. 1b).

One may now attempt to extract a general quantitative characterization of the onset of merging, using a criterion based on a normalized vortex core size, similar to the one discussed in the previous chapter (Eq. (6)). A first attempt to define a core size, often used in previous studies, can be made using the vortex area S, which in our scalings is a constant. This gives a core radius of $\sqrt{S/\pi}$. However, the corresponding critical ratio $\sqrt{(S/\pi)}/L_c$ is found here to vary in a range between 0.30 to 0.35 for the parabolic family. This means that the merging criterion with this definition of core size is very dependent on the profile of vorticity and does therefore not seem to be useful to the case of non-uniform patches.

A more suitable definition of core radius may be obtained using the partial angular impulse J for each vortex:

$$J = \int_S \omega(\mathbf{r}) |\mathbf{r}|^2 dS, \tag{17}$$

where integration is performed over the area of a single vortex, and $\mathbf{r}$ is measured from its center O_i, and not from O. The simplest length scale that may be extracted from any vorticity distribution,

axisymmetric or asymmetric, and which we call l_ω in the following, is the square root of the second moment of vorticity, *i.e.* the angular impulse, divided by its zeroth moment, *i.e.* the circulation:

$$l_\omega = \sqrt{J/\Gamma}. \tag{18}$$

It is a measure for the spatial extent of a given vorticity distribution. For the axisymmetric Gaussian-like vortices of Eq. (14), this quantity is given by

$$l_\omega = \sqrt{\frac{1}{\alpha} - \frac{\exp(-\alpha)}{1-\exp(-\alpha)}}, \tag{19}$$

whereas for the parabolic distributions (Eq. (15)) it reads

$$l_\omega = \sqrt{\frac{3-2\alpha}{6-3\alpha}}. \tag{20}$$

The evolution of l_ω with the vortex separation distance L, obtained by decreasing the latter, is shown in Fig. 9, for different initially parabolic vorticity distributions. The circles in Fig. 9 mark the values at the critical distance L_c. (For large values of L one would recover the axisymmetric quantity.) While there is a certain variation in the vicinity of the critical distance for the almost uniform case, l_ω depends only weakly on the distance L for profiles with relatively small vorticity at the vortex boundary (here for $\alpha = 0.9, 1$). The strongest deformations of the streamlines appear close to the vortex boundary and, the smaller the vorticity is in this region, the less the geometrical deformation modifies the angular impulse J.

Tables I and II summarize the critical values (where exchange of stability occurs for the equilibrium state), for both the parabolic and Gaussian-like initial vorticity distributions. Note that for both solution families an almost uniform vorticity distribution has been considered, with $\alpha = 10^{-4}$ for the parabolic profile and $\alpha = 10^{-3}$ for the Gaussian profile. (In the present model, the Green's integral is expressed as a vorticity integral and hence the relationships (14) and (15) must be inverted, which makes the parameter $\alpha = 0$, corresponding to a strictly uniform vortex, a singular value in our solution procedure). Tables I and II also give the non-dimensional core size l_ω/L_c, calculated at the critical distance between the vortex centers. For the parabolic solution family, this parameter varies very little; the expression

$$l_\omega/L_c = 0.218 \pm 0.010, \qquad \text{(theoretical)} \tag{21}$$

represents the results for the entire set of parabolic distributions, from the uniform case to the one with zero vorticity at the outer boundary of the vortex. The variations with α are found to

be much smaller than those of the quantity $\sqrt{(S/\pi)}/L_c$. The quantity l_ω/L seems to be a more natural choice when considering a quantitative criterion for the merging of real vortices, since its definition uses global properties of the vortex, instead of the characteristics of the contour of the patch as in previous studies.

For the theoretical Gaussian-profile solutions, the dimensionless quantity l_ω/L_c seems to behave less favorably. It is found to vary significantly, decreasing with increasing α (Table II). Nevertheless, the critical ratios obtained for moderate α (columns 3 and 4 in Table II) are in good agreement with the result in Eq. (21). Due to the particular shape of the Gaussian vorticity distribution (cf. Fig. 7) the region containing relatively small vorticity values increases with α, and the theoretical model appears to be sensitive to the details of this outer low-vorticity distribution. Also, as explained above, higher α-values in the Gaussian profiles may be rather unphysical, leading to low values of the angular impulse J, and consequently to a low l_ω, at criticality. In order to illustrate this the idea that the model works better when the vorticity is more uniformly distributed over the entire region of the vortex, some computations have also been performed for a pair of initially compact vortices (16), for which the vorticity is zero at the boundary. For $\alpha = 0.1$ (the corresponding profile is depicted in Fig. 7), the critical values are

$$L_c = 3.049,\ \delta_c = 0.077,\ (l_\omega/L)_c = 0.214,$$

and the theoretical value (21) is almost retrieved. Note that the minimum separation distance δ between the two vortices at criticality is close to zero. When increasing α in (16), the vortices touch before a bifurcation point is detected (in our model, only stationary bifurcation points which occur for $\delta \geq 0$ are meaningful).

In section II, the experimental core size a defined for a Lamb-Oseen vortex (Eq. (1)), was considered. For an axisymmetric unbounded Gaussian vortex, a is equal to l_ω. Assuming that the angular momentum of each vortex is close to the one of an axisymmetric one up to the onset of merging, the experimental result given in Eq. (6) is equivalent to

$$(l_\omega/L)_c = 0.24 \pm 0.01, \qquad \text{(experimental)} \tag{22}$$

which is reasonably close to the critical value given in Eq. (21). This indicates that the definition of the core size using the angular momentum is well adapted to the merging of vortices with distributed vorticity. With this result, a refined criterion for merging may be formulated, which generalizes and adds precision to previous results:

Two identical distributed vortices will merge into a single one, if the ratio of their characteristic vorticity radius l_ω (as defined in Eq. (18)) and their separation distance exceeds a critical value.

The numerical value of the critical ratio lies somewhere between 0.21 and 0.25, according to Eqs. (21) and (22).

Figure 10 shows a collection of the critical ratios l_ω/L_c obtained for the two families of non-uniform vortices considered in this paper. The experimental value is also plotted for comparison. It seems that theoretical predictions are consistently underestimating the critical value. The theoretical model captures the first instability of an inviscid equilibrium configuration, and it may therefore not be too surprising that the corresponding critical ratios are below the one which may be experimentally observed at merging. Indeed, the fact that the equilibrium state becomes unstable may not necessarily be equivalent to the onset of merging; it may be linked to a subsequent bifurcation of the flow (at a higher l_ω/L_c), which our numerical procedure is unable to capture. On the other hand, the fact that the critical values from experiment and theory are nevertheless close, lends some credit to the idea that the loss of stability of the Euler equilibria is at least a precursory sign of actual merging.

Other criteria have previously been considered, and it is worthwhile comparing them to the present results. One merging criterion is based on the ratio between the critical separation distance L_c and the vortex patch diameter d (for non-circular patches, an equivalent diameter can be calculated using the patch area). For uniform vorticity patches, the work of Saffman and Szeto [17] yields a critical ratio $L_c/d = 1.58$, below which no stable equilibrium state is found. It is easily checked that, for a uniform patch of radius r, $l_\omega = r/\sqrt{2}$. With this, the present calculations for the (almost) uniform case yield $L_c/d = 1.55$, which is in good agreement with the previous result. Inversely, Saffmann and Szeto's result implies $l_\omega/L_c = 0.224$ for their case, which is consistent with the criteria found here. However, as noted earlier, as soon as the vorticity profile is no longer constant across the patch, the numerical values of L_c/d vary significantly, making this parameter less useful for a 'universal' merging criterion.

In vortex merger experiments performed by Fine *et al* [30], using electron plasmas, a merging criterion based on a length scale

$$l_1 = \frac{1}{\Gamma}\int \omega(\mathbf{r})\,|\mathbf{r}|\,dS,$$

calculated with the first moment of vorticity was proposed. The parameter $L_c/3l_1$ was considered, which, for uniform patches, corresponds to the ratio between separation distance and patch diameter. When calculating this quantity for the present theoretical results, one finds values between

1.57 and 1.76 in the case of parabolic profiles, whereas the experimental result in (22) translates into $L_c/3l_1 = 1.57$ ($l_1 = a\sqrt{\pi}/2$ for a Gaussian vortex (1)). These results are well well within the range of critical values given in [30]. Considering on the other hand, as done throughout this paper, the ratio between a characteristic core radius and the vortex separation distance, but using l_1 instead of l_ω, the critical values in (21) and (22) become $(l_1/L)_c = 0.20$ and $(l_1/L)_c = 0.21$, respectively, with the result for the Gaussian distributions again being lower. On the whole, the merging criterion based on the first moment of vorticity behaves very similar to the one using the angular momentum. Again, little variation is found with different non-uniform vorticity profiles, after accounting for the limitations of our theoretical model. Nevertheless, with the angular momentum being an invariant of inviscid vortex motion, it seems more natural to use the second moment of the vorticity distribution for the purpose of defining a general criterion for vortex merging.

V. CONCLUSION

In this paper, we have performed an extension of the theoretical analysis of Saffman and Szeto [17], concerning the two-dimensional interaction of co-rotating vortices, to the case of patches with different types of non uniform vorticity. The resulting algorithm finds Euler solutions with two vortices, containing concentric patches of uniform vorticity. The profiles of vorticity were varied from parabolic and truncated Gaussian to nearly uniform.

Earlier studies have shown that the two vortices do not remain separated, but merge into a single final vortex, if the characteristic size of the vortex core exceeds a certain fraction of their separation distance. This qualitative behaviour was also observed in the present theoretical study, where the solutions become unstable when the distance is decreased beyond a certain limit. However, it was found that the numerical value for the critical core size-to-separation distance ratio varies significantly with the vorticity profile, when the core radius is simply calculated from the area of the vortex, as done previously [17]. A new definition of characteristic core size, involving the angular momentum of vorticity, was tested, and much less dependence on the particular vorticity profile of the initial vortices was observed. A refined merging criterion, using this more general definition of core size, is therefore proposed, which is believed to be applicable with good numerical accuracy for a large class of distributed vortices.

The merging of two co-rotating vortices has also been investigated experimentally at different Reynolds numbers. In a real flow with non-zero viscosity, the core size evolves due to diffusion

of vorticity. The vortex pair evolution is therefore characterized by the existence of three stages: a first viscous stage, where the square of the core size increases linearly in time, without merging followed by a second stage, where the two vortices merge on a convective time scale; the diffusion of filaments of vorticity into a final axisymmetric distribution of vorticity characterizes the third stage. The transition between the first two stages is obtained for a critical core size, which can be calculated quite accurately from the series of experiments at different Reynolds numbers, using the assumption of different stages of vortex evolution. From these experiments, the numerical value of the critical core size (using the new definition) is within 10% of the critical ratio obtained in the theoretical study. The latter is believed to slightly underestimate this limit, since, by construction, not all conceivably stable configurations are possible in the present formalism. Nevertheless, the agreement between the two results is rather satisfactory.

The present study has led to the identification of a dimensionless quantity characterizing the geometry of symmetric co-rotating vortex pairs, which proved useful in determining the merging characteristics of such vortex systems, independently of their detailed vorticity distribution. Both the theoretical and experimental procedures can in principal be applied to systems of non-identical co-rotating vortices, and a similar merging criterion is expected to hold for these cases.

REFERENCES

[1] Y. Couder, J. M. Chomaz, and M. Rabaud, "On the hydrodynamics of soap films," Physica D **37**, 384 (1989).

[2] P. Tabeling, S. Burkhart, O. Cardoso, and H. Willaime, "Experimental study of freely decaying two-dimensional turbulence," Phys. Rev. Lett. **67**, 3372 (1991).

[3] J. C. Mc Williams, "The vortices of two-dimensional turbulence," J. Fluid Mech. **219**, 361 (1990).

[4] J. Jimenez, H. K. Moffatt, and C. Vasco, "The structure of the vortices in freely decaying two-dimensional turbulence," J. Fluid Mech. **313**, 209 (1996).

[5] E. Hopfinger, F. Browand, and Y. Gagne, "The structure of turbulence in homogeneous and stratified rotating fluids," J. de Mécanique Théorique et Appliquée **21**, Numéro Spécial (1983).

[6] A. Vincent and M. Meneguzzi, "The spatial structure and statistical properties of homogeneous turbulence," J. Fluid Mech. **225**, 1 (1991).

[7] A. Maurel and P. Petitjeans (Eds.), *Vortex Structure and Dynamics*, Lecture Notes in Physics **555**, Springer Verlag (2000).

[8] P. G. Drazin and W. H. Reid, *Hydrodynamic Stability*, Cambridge University Press (1981).

[9] P. Huerre and M. Rossi, "Hydrodynamic instabilities in open flows," in *Hydrodynamics and Nonlinear Instabilities*, edited by C. Godrèche and P. Manneville, pp. 81-294, Cambridge University Press (1998).

[10] P. G. Saffman, *Vortex Dynamics*, Cambridge University Press (1992).

[11] P. Meunier and T. Leweke, "Merging and three-dimensional instability in a corotating vortex pair," in *Vortex Structure and Dynamics*, edited by A. Maurel and P. Petitjeans, Lecture Notes in Physics **555**, pp. 241–251, Springer Verlag (2000).

[12] L. Ting and C. Tung, "Motion and decay of a vortex in a nonuniform stream," Phys. Fluids **8**, 1039 (1965).

[13] M. V. Melander, N. J. Zabusky, and J. C. McWilliams, "Symmetric vortex merger in two dimensions: causes and conditions," J. Fluid Mech. **195**, 303 (1988).

[14] N. K. R. Kevlahan and M. Farge, "Vorticity in two-dimensional turbulence: creation, stability and effect," J. Fluid Mech. **346**, 49 (1997).

[15] O. Agullo and A. D. Verga, "Exact two vortices solutions of Navier-Stokes equations," Phys. Rev. Lett. **78**, 2361 (1997).

[16] D. G. Dritschel, "The stability and energetics of corotating uniform vortices," J. Fluid Mech. **157**, 95 (1985).

[17] P. G. Saffman and R. Szeto, "Equilibrium shapes of a pair of equal uniform vortices," Phys. Fluids **23**, 2339 (1980).

[18] D. G. Dritschel, "A general theory for two-dimensional vortex interactions," J. Fluid Mech. **293**, 269 (1995).

[19] E. A. Overman, "Steady-state solutions of the Euler squations in two dimensions. II. Local analysis of limiting V-states," SIAM J. Appl. Math. **46**, 765 (1986).

[20] D.W. Waugh, "The efficiency of symmetric vortex merger," Phys. Fluids A **4**, 1745 (1992).

[21] R. Robert and J. Sommeria, "Statistical equilibrium states for two-dimensional flows," J. Fluid Mech. **229**, 291 (1991).

[22] B. Turkington, "Statistical equilibrium measures and coherent states in two-dimensional turbulence," Comm. Pure Appl. Math. **52**, 781 (1999).

[23] U. Ehrenstein and M. Rossi, "Equilibria of corotating nonuniform vortices," Phys. Fluids **11**,

3416 (1999).

[24] P. Meunier and T. Leweke, “Three-dimensional instability during vortex merging,” Phys. Fluids **13**(10) (2001), in press.

[25] T. S. Lundgren, “Strained spiral vortex model for turbulent fine structure,” Phys. Fluids **25**, 2193 (1982).

[26] A. J. Bernoff and J. F. Lingevitch, “Rapid relaxation of an axisymmetric vortex,” Phys. Fluids **6**, 3717 (1994).

[27] D. G. Dritschel and N. J. Zabusky, “On the nature of vortex interactions and models in unforced nearly-inviscid two-dimensional turbulence,” Phys. Fluids **8**, 1252 (1996).

[28] B. J. Bayly, “Three-dimensional centrifugal-type instability in an inviscid two-dimensional flow,” Phys. Fluids **31**, 56 (1988).

[29] H. B. Keller, “Numerical solution of bifurcation and nonlinear eigenvalue problems,” in *Application of Bifurcation Theory,* edited by P. H. Rabinowitz, pp. 359-384, Academic Press (1977).

[30] K. S. Fine, C. F. Driscoll, J. H. Malmberg and T. B. Mitchell, “Measurements of symmetric vortex merger,” Phys. Rev. Lett. **67**, 588 (1991).

TABLES

α	1	0.99	0.95	0.9	10^{-4}
$\omega_{min}/\omega_{max}$	0	0.01	0.05	0.1	≈ 1
L_c	2.840	2.849	2.881	2.916	3.288
δ	0	≈ 0	0.010	0.077	0.475
l_ω	0.591	0.594	0.607	0.622	0.751
l_ω/L_c	0.208	0.208	0.211	0.213	0.228

TABLE I: Critical values for parabolic profiles.

α	4.60	3.00	2.30	10^{-3}
$\omega_{min}/\omega_{max}$	0.01	0.05	0.1	≈ 1
L_c	2.734	2.814	2.882	3.287
δ	0.016	0.038	0.085	0.496
l_ω	0.466	0.542	0.589	0.750
l_ω/L_c	0.171	0.193	0.204	0.228

TABLE II: Critical values for Gaussian profiles.

FIGURE CAPTIONS

FIG. 1: Visualization of the two-dimensional merging of two co-rotating vortices at $Re \approx 2000$. (a) $t^* = 1.1$, (b) $t^* = 1.7$, (c) $t^* = 2.0$, (d) $t^* = 3.1$.

FIG. 2: Evolution of the separation distance between the two vortex centers. The determination of the onset of merging from such measurements is necessarily subjective.

FIG. 3: "Merging time" as function of the Reynolds number for a separation distance fraction $x = L/L_o = 0.6$.

FIG. 4: Experimental critical core radius as function of the limit fraction x of the separation distance. The straight line corresponds to the average $a_c/L_o = 0.24$ of the critical ratios.

FIG. 5: Vorticity distribution at the critical core size for $Re = 1506$. Isocontours are separated by 0.3 s^{-1}.

FIG. 6: Geometry of the symmetric vortex pair in a rotating frame.

FIG. 7: Axisymmetric vorticity distribution for $\omega_{min}/\omega_{max} = 0.05$. —— : Gaussian profile; - - - - : parabolic profile. -.-. : compact vortex distribution, $\alpha = 0.1$.

FIG. 8: Streamlines for an equilibrium vortex pair at the point of exchange of stability. (a) Parabolic profile with $\alpha = 1$; (b) constant-vorticity patch; (c) Lamb-like profile with $\alpha = 2.25$.

FIG. 9: The value of l_ω as a function of distance L for parabolic vorticity distributions. —— : $\alpha = 1$; $-\cdot-\cdot$: $\alpha = 0.9$; - - - - : $\alpha = 10^{-4}$. $\circ$: values at critical distance L_c.

FIG. 10: The value of quantity l_ω/L_c, as function of $\omega_{min}/\omega_{max}$. $\triangle$: parabolic profiles; $*$: Gaussian profiles. The dashed line corresponds to the experimental value.

(a) 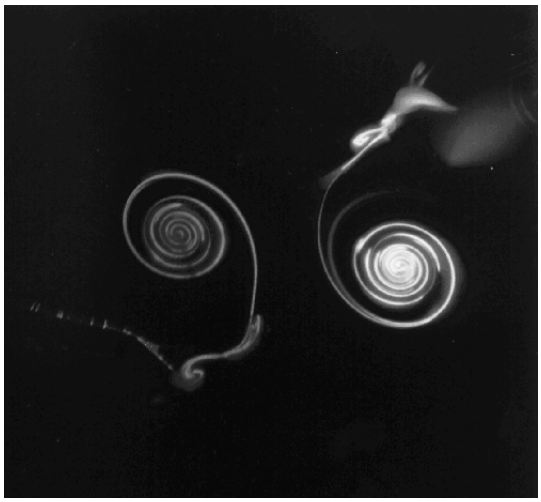

(b) 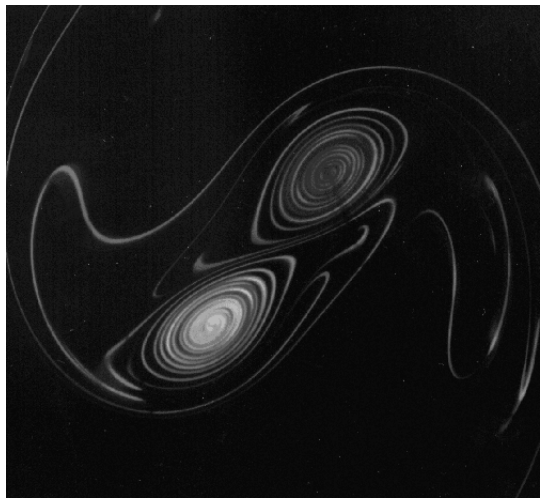

(c) 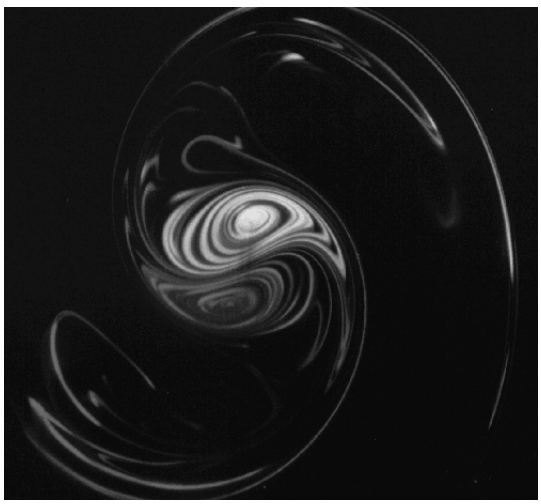

(d) 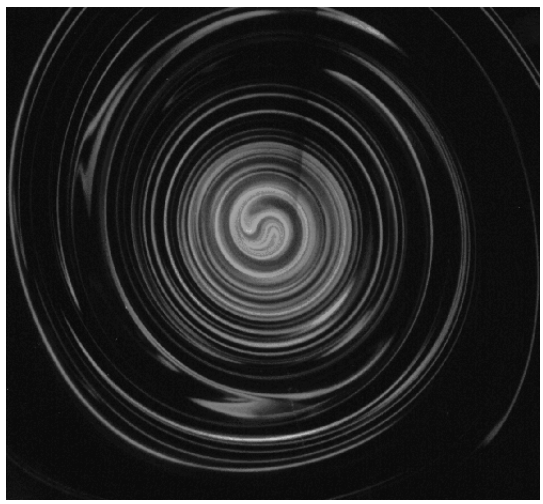

Figure 1, Meunier, Physics of Fluids

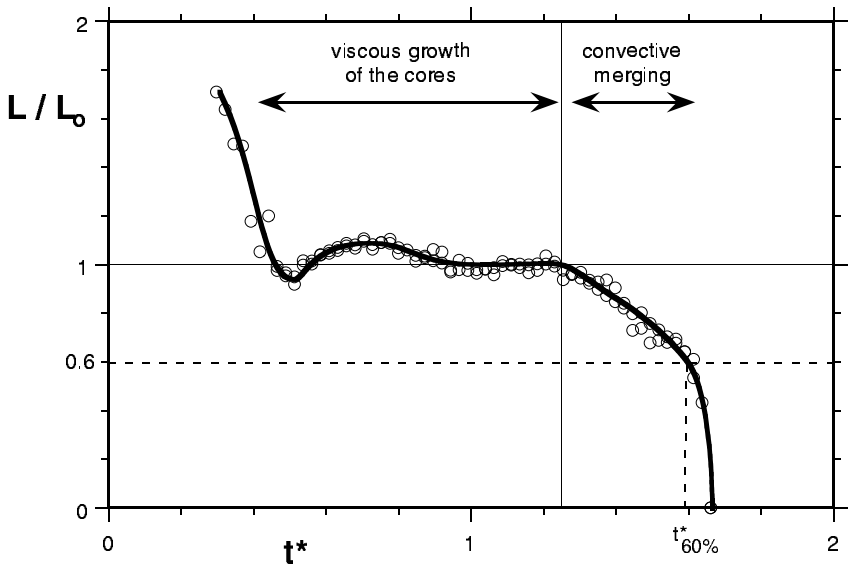

Figure 2, Meunier, Physics of Fluids

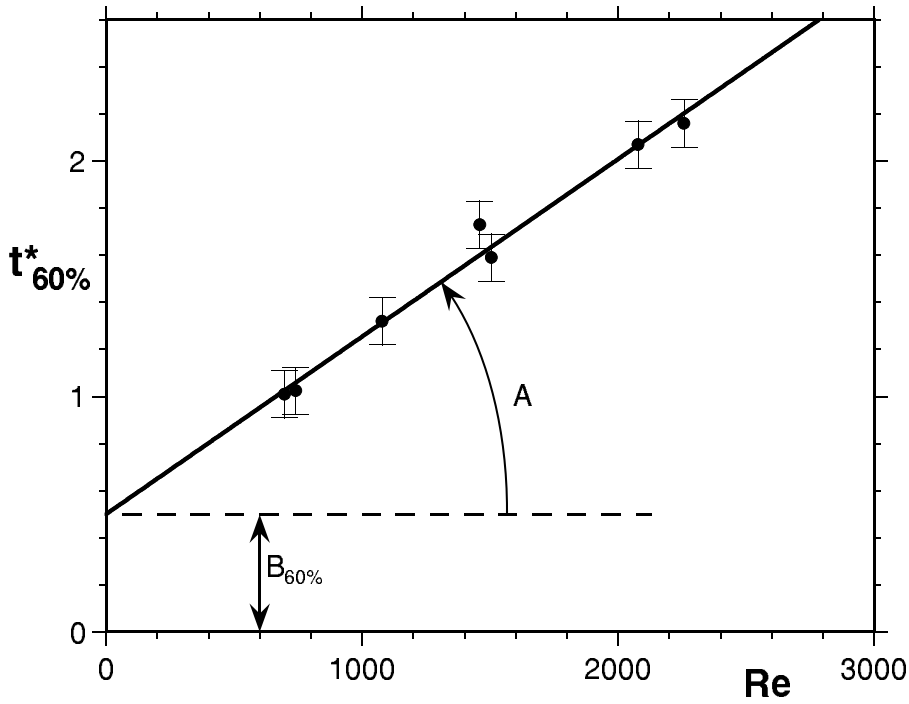

Figure 3, Meunier, Physics of Fluids

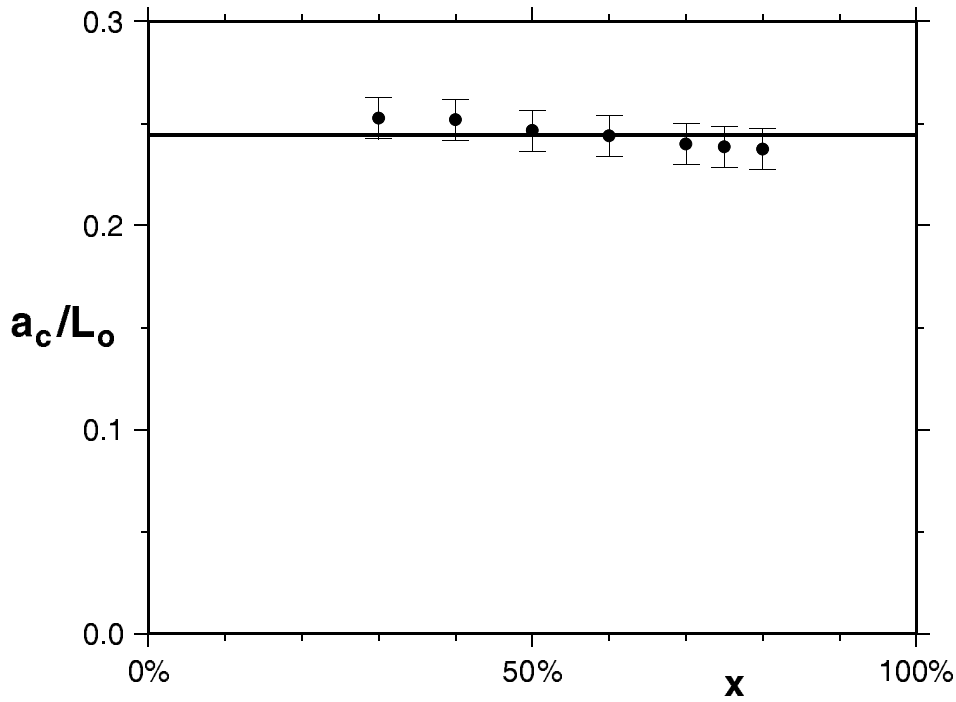

Figure 4, Meunier, Physics of Fluids

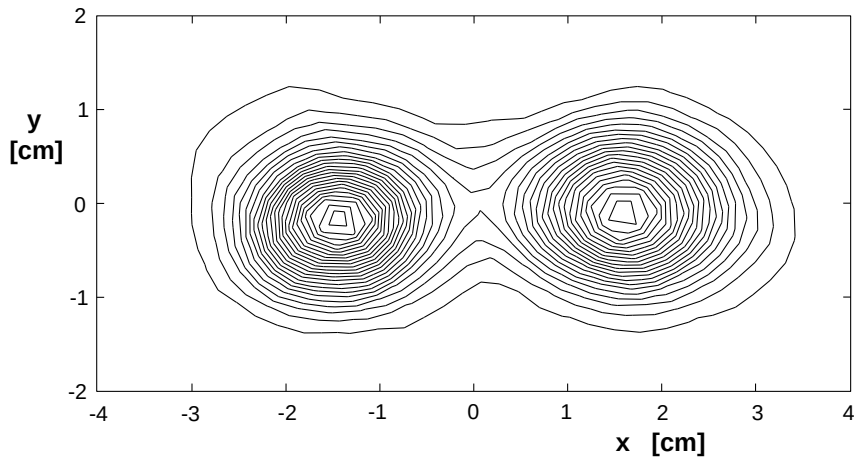

Figure 5, Meunier, Physics of Fluids

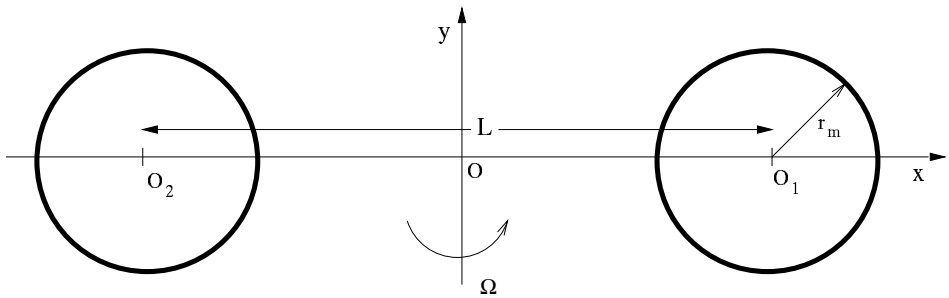

Figure 6, Meunier, Physics of Fluids

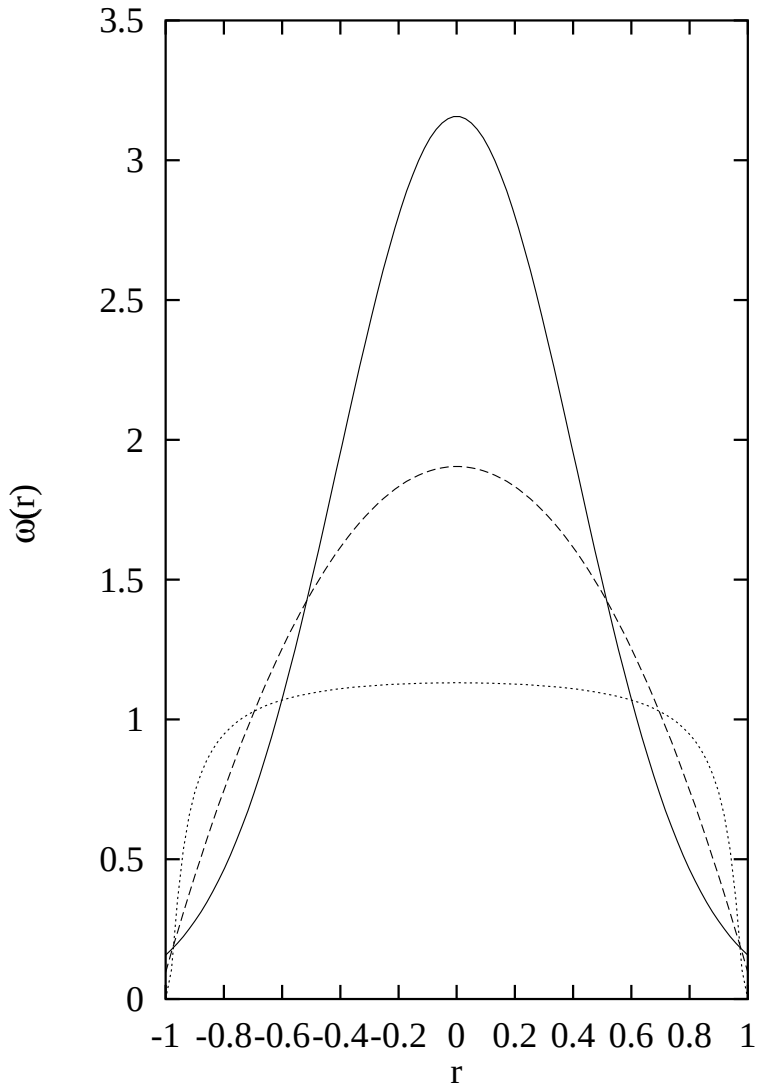

Figure 7, Meunier, Physics of Fluids

(a)

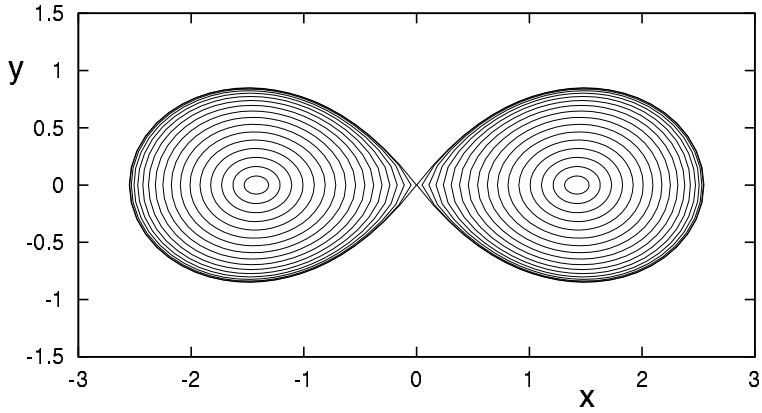

(b)

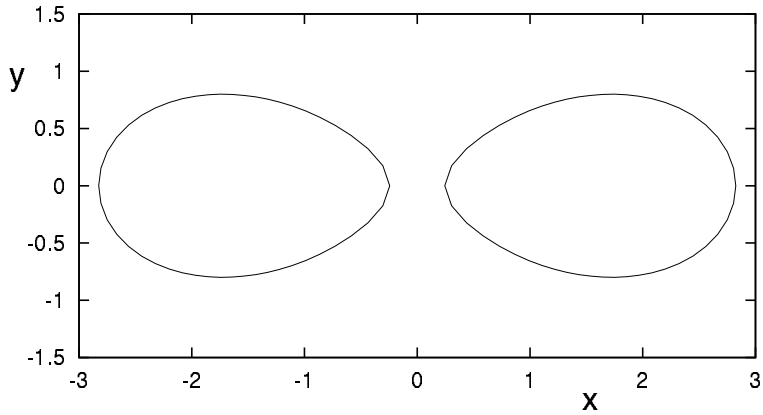

(c)

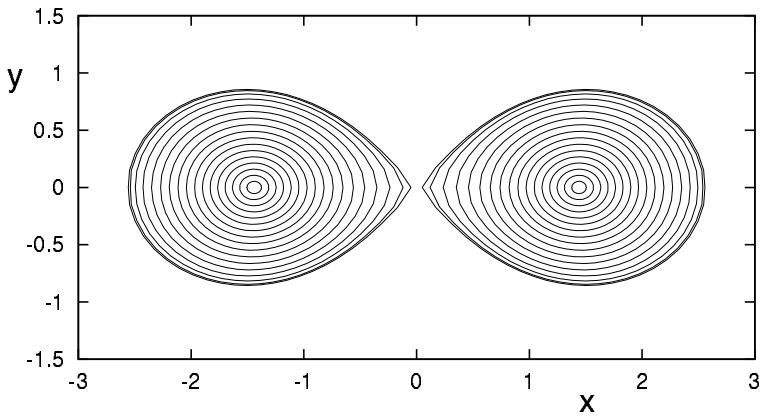

Figure 8, Meunier, Physics of Fluids

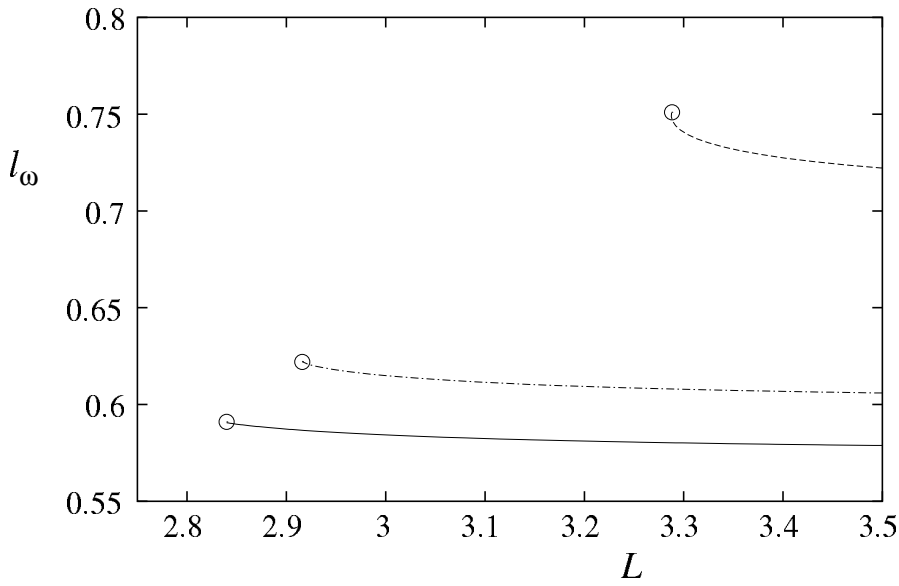

Figure 9, Meunier, Physics of Fluids

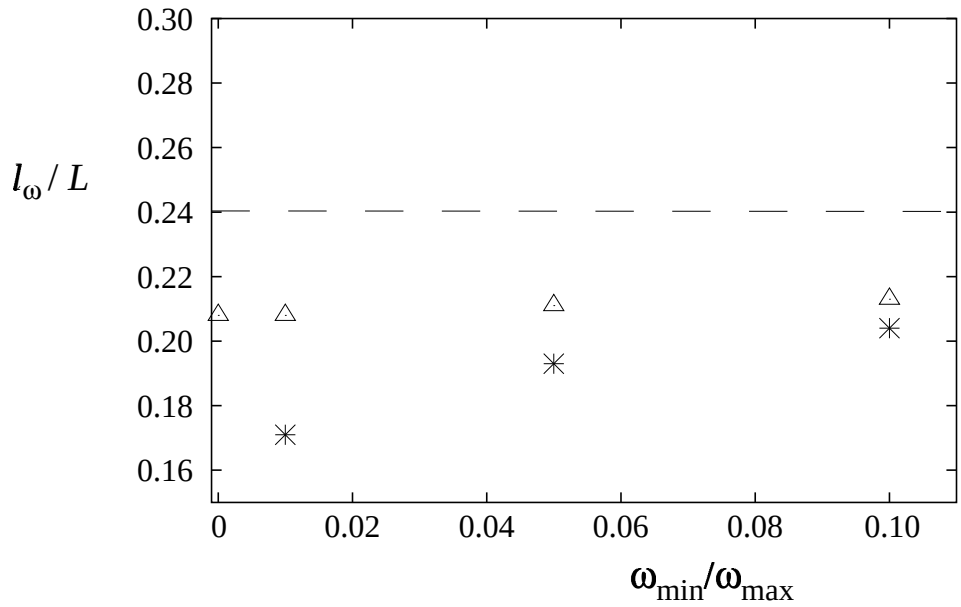

Figure 10, Meunier, Physics of Fluids